

A deep learning approach to detect the electroencephalogram-based cognitive task states

Hitesh Yadav* and Surita Maini

Department of Electrical and Instrumentation Engineering, Sant Longowal Institute of Engineering and Technology, Longowal, Sangrur, Punjab, India

Received: 01-July-2022; Revised: 21-March-2023; Accepted: 24-March-2023

©2023 Hitesh Yadav and Surita Maini. This is an open access article distributed under the Creative Commons Attribution (CC BY) License, which permits unrestricted use, distribution, and reproduction in any medium, provided the original work is properly cited.

Abstract

Cognitive abilities are responsible for performing various simple and complex activities that affect a person's mental performance. These are also responsible for different day-to-day actions in human life. In the past few years, studies on cognitive ability, mental performance, and mindfulness meditation have been seen more frequently. The electroencephalogram (EEG) is an effective technique to study brain dynamics while executing any cognitive task and leads to new possibilities in the brain-computer interface (BCI) field. In this study, twenty-seven (27) healthy subjects performed a designed cognitive task having three different states (i.e., rest, meditation, and arithmetic) to stimulate the brain's cognitive functions. BIOPAC-MP-160 has been used for the EEG signal acquisition of the designed cognitive task according to the international 10-20 data acquisition system. The EEGLAB has been used to visualize, pre-process, filter, and removal of noise from the data. Then phase-amplitude coupling is performed to extract the features. After completing the feature extraction, the classification has been performed by three different deep learning approaches, i.e., sequential convolutional network (SCN), multi-branch convolutional network (MBCN), and multi-branch convolutional network-bidirectional long short-term memory network (MBCN-Bi-LSTM). The performance of the different classifications model has been estimated in terms of accuracy, precision, F1 score, and recall. The results demonstrated that MBCN-Bi-LSTM performs better than the SCN and MBCN, with a significant improvement in accuracy of 97.99%. The comparative analysis of the previously used deep learning and machine learning approaches to classify the EEG signal of different brain states substantially indicates that the proposed MBCN-Bi-LSTM model performs better in terms of accuracy and error rate. Also, the computational execution time of the proposed MBCN-Bi-LSTM is found to be less than the previous methods. The proposed classification approach may be utilized in future research to classify the various physiological signals.

Keywords

BCI, EEG, Deep learning, Classification, Cognitive task, Mental state classification.

1.Introduction

Brain-computer interface (BCI) is an important topic for researchers and the scientific community, as indicated by the abundance of research and study materials in the field. The purpose of the BCI is to allow interaction with any device or computer via brain signals. According to this definition, BCI strives to collect the brain signals using sensors, analyze and process these received signals, and then extract features to operate any device. Simply, it is a link between the brain and the device. The user can control the device by using the brain's neural activities.

BCI was first developed for biomedical applications to enable physically impaired persons to move around by substituting for lost motor functions [1]. Nowadays, it includes non-medical applications as well [2, 3]. Newer areas of BCI research include lie detection, drowsiness detection, cognitive studies, motor imagery, virtual reality, video games, driver fatigue detection, stress detection, and many more. From these applications, cognitive ability is important to understanding brain functioning. Cognitive ability depends from person to person and is essential in controlling various mental activities [4]. BCI research has been accelerated by technological advances enabling processing and observing mental and cognitive activities [5]. Any cognitive task reveals how the person thinks, utilizes,

*Author for correspondence

and manipulates the information and how his brain learns to respond quickly to any given command. Cognitive neuroscience has grown tremendously over the last few decades. Clinical experiments developed many neuroimaging techniques in different BCI studies throughout the decades. The advancement and expansion of non-invasive data acquisition techniques, electrode development, and feature extraction techniques are the fields of neuroscience where remarkable improvements have been achieved [6].

Various data acquisition techniques are available to extract meaningful information for BCIs. Electroencephalogram (EEG), functional magnetic resonance imaging (fMRI), positron emission tomography (PET), and magnetoencephalography (MEG) are some of the available techniques. EEG is a non-invasive technique where one can extract signals from the brain and use them for further processing to find valuable information. In the EEG, one can quantify the electrical signal generated by the physio-electrical activity of the brain. The EEG waveform varies with the electrode locations, and it is a complex pattern compared to other vital body signals such as electrocardiography (ECG). It is an inexpensive, affordable, safe, and readily available technique [7]. EEG captures the various neural activities due to different cognitive tasks, motor imagery tasks, and activities due to different mental workloads/stress [8, 9]. These changes are directly related to the subject's present state, whether it is stressed, calm, or having any other illness. For patients with mental and behavioral diseases such as autism, the accurate classification of neuronal activities plays a vital role in their treatment [10]. Further, healthy subjects can also improve their cognitive performance; that's why cognitive analysis is essential. The classification of different mental states using EEG is also helpful for the early detection of mental stress that can prevent hypertension, diabetes, and heart attack-like fatal conditions [11].

EEG-based cognitive and behavior assessment needed time and frequency domain information over extended scalp areas [12]. Analyzing the EEG signal manually is time-consuming, requires proper EEG background knowledge, and is expensive. Since this field started, various machine-learning and deep-learning methods have played a crucial role in the BCI literature for mental state classification [13, 14]. Convolutional neural networks (CNN) attracted researchers due to their ability to extract high-level

features and classification accuracy enhancement for different signals [15]. Automated EEG signal analysis decreases the possibility of human error and is relatively faster than conventional methods [16, 17]. Different EEG-based imagery classifications also frequently use deep learning techniques [18]. Various deep learning approaches, such as layer-based CNN models [19], multi-layer perceptron (MLP) [20], capsule network [21], and some machine learning approaches [22], have been utilized recently for EEG signal classification. Generally, the classification performances have been compared based on accuracy. Few studies are available where the precision, F1 score, and recall were considered. Except this, most of the deep learning architecture utilized the raw EEG data as the input, and very few used feature extractions before the classification. Most of the studies have been performed on the available online datasets, and very few have performed real-time data acquisition. All these factors motivated the authors to work in this field and to develop an EEG-based BCI system using a cognitive task. Thus the development of a method that can distinguish different mental states has become the central idea of this research. In our study, real-time data has been used, and the deep learning approach is utilized to distinguish a cognitive task's different mental states. We have performed feature extraction instead of directly fed signals to the CNN to get better results. The authors designed a cognitive task that processed EEG signals. We used sequential convolutional network (SCN), multi-branch convolutional network (MBCN), and multi-branch convolutional network-bidirectional long short-term memory network (MBCN-Bi-LSTM) models to classify the EEG signal using the phase-amplitude coupling (PAC) feature extraction method. Motivated by the previous research [23], where two different models were proposed and applied to the datasets to classify various cognitive tasks, we applied such models to our cognitive task dataset and compared the result with our proposed MBCN-Bi-LSTM model. Lastly, a comparison has been made between the approaches used in this study and previously used methods. The main contributions of this study are:

- Designed a cognitive task having three different states, i.e., rest, meditation, and arithmetic.
- Acquired the EEG data of the cognitive task using BIOPAC-MP-160.
- Data pre-processing has been done using EEGLAB.
- The classification models mentioned above classify the cognitive task's different states.

- The comparison of these models with conventional methods used previously based on performance parameters

The paper organization is as follows: Section two describes the literature review. Section three includes the methodology and proposed classification approaches. Section four discusses the result, and section five is the discussion consisting of study limitations. Lastly, section six consists of the conclusion and future work.

2.Literature review

Cognitive abilities evaluate the human brain's performance while experiencing different situations. A person's ability to learn new things, process these things, concentrate, analytical knowledge, reasoning, attention, immersion, etc., influences the person's cognitive approach and affects daily life. An efficient cognitive task classification requires an effective feature extraction technique in any BCI system. The acquired EEG signal can be fragmented into different frequency bands, starting from delta to gamma, and these frequency bands are associated with different mental conditions. The neural oscillations produced in different brain regions have been directly correlated with different cognitive activities. Independent component analysis (ICA) is a typical method except for these other beneficial feature extraction methods like power spectral density (PSD), mean absolute value, wavelet transform (WT), and short-time Fourier transform (STFT) that are used in the time domain and frequency domain feature extraction [24]. Other parameters that affect cognitive task performances are alpha peak frequency [25], alpha-theta cross-frequency correlation [26], task engagement index, etc. [27]. Different literature is available for classifying various types of mental activities using EEG. Dutta et al. [28] used multivariate autoregressive (MAR) model-based features to classify three cognitive tasks by the least square support vector machine (LS-SVM) classifier. Noshadi et al. [29] classified five different mental states using K-nearest neighbor (K-NN) and linear discriminant analysis (LDA) classifiers. PSD-based features have been used for the LDA classifier to classify the mental states of six subjects [30]. Gaurav and Kumar [31] classified three different cognitive tasks using MLP and SVM. In this study, the EEG signals were recorded for 41 subjects. Qayyum et al. [32] obtained EEG signals from 32 subjects during different multimedia learning tasks. The WT and CNN have been utilized for feature extraction. Zhang et al. [33] proposed a three-dimensional (3-D) CNN

to classify mental workload-based arithmetic tasks in 20 subjects. Similarly, the four levels of cognitive load from 13 subjects have been classified by 3-D CNN [34]. Recently a long short-term memory network (LSTM) and stacked auto-encoder (SAE) combined to differentiate five imagery tasks [35]. The deep learning method was applied to the anesthetic patient's dataset for classifying various states of a cognitive task [36]. Deep CNN is used to detect displacement-related insights from the raw EEG signal [37]. A new approach proposed a compact CNN for EEG-based BCI called EEG-Net to extract features [38]. A CNN approach with stacked auto-encoders and LSTM has been used for time series classification [39]. Some researchers proposed a unique deep learning technique having MLP and CNN to distinguish the EEG and electromyogram (EMG) signals with minimum computational cost [40]. The suitable network parameters can be estimated using an optimal multi-objective method. The signal characteristics have been extracted and used to classify different states of the cognitive task. Samanta et al. [41] proposed A multiplex weighted graph method to classify a motor imagery task. An auto-encoder-based characteristics detection technique extracts the desired features for classifying EEG signals. Further, a common spatial pattern (CSP) based feature extraction technique was proposed during the training for artifact-related issues, and a convolution LSTM model was used for classification [42]. The STFT algorithm has been utilized in many studies to transform the time domain pattern into its frequency spectrums. This information was provided to the CNN architecture to extract discriminative features from the EEG signal [43]. Deep learning methods revolutionized the classification technique domain. They can detect the features automatically from a given input signal and offer higher classification accuracy than the machine learning approach, where the feature extraction process is mandatory [44]. Amin et al. [45] extracted features of EEG signals using a multi-layer CNN model. A fusion technique has been used to merge various CNN models and classify the EEG signal. A CNN-based transformer model has been proposed to classify the online available EEG dataset where three and four-class classifications have been done. The results are impressive, but the system complexity can be minimized in future research. Altuwarijri and Muhammad [46] proposed subject-based EEG classification, where different channel locations were suitably selected for different subjects. The proposed deep learning architecture improved the classification accuracy significantly. Farsi et al. [47] proposed a

method for EEG classification of two distinct brain states, i.e., normal and alcoholic. In this study, the classification was performed by the CNN-Bi-LSTM model. A promising approach, i.e., cross-frequency coupling (CFC), is a tool that includes information on various frequencies in different brain regions. Such interaction between different bands of frequencies gives us crucial information about the system that controls neural activities across different frequency bands to differentiate the cognitive task states [48]. Research shows how CFC correlates with different frequency bands and generates the distinguishing features for various cognitive task conditions [49]. PAC is a method of finding CFC where the low-frequency phases modulate the amplitudes of high frequencies. Mean vector length, modulation index (MI), and phase values are some indicators used to estimate PAC values [50]. The authors proposed a technique to find the PAC values using the Kullback-Leibler (KL) transformation method [51]. Hulsemann et al. [52] compared various techniques to classify different cognitive tasks, and the results demonstrated that PAC performs better.

From the literature, it can be seen that several researchers use hand-crafted feature extraction and conventional machine-learning approaches while mostly using deep learning-based techniques for cognitive/mental task classification. In recent years, deep learning-based methods have increased cognitive/mental task classification accuracy. Therefore, we proposed a deep learning-based approach to classify a designed cognitive task. To achieve greater classification accuracy, the artifact removal, pre-processing, and feature extraction steps have been performed by EEGLAB and PAC methods.

3. Methodology

The flow diagram of the methodology is shown in Figure 1. The different subsections of methodology, i.e., cognitive task design and data acquisition, pre-processing, feature extraction, and classification models, are described in this section.

3.1 Cognitive task design

The authors have designed a specific cognitive task based on textbooks and research papers. Working minds, a book for cognitive task study by Crandall et al. [53], and a handbook on cognitive task design: Human Factors and Ergonomics by Salmon et al. [54], helped us with the cognitive task design. All the factors, conditions, benefits, and drawbacks from the literature were considered to design the task. The

designed cognitive task consists of three states, i.e., rest, meditation, and arithmetic. Five minutes of data were collected for each condition. At rest, the test subjects were asked to close their eyes, feel free and de-attach themselves from the outside world interrupts and let go of thoughts. In the induced meditation condition, subjects listened to an Om chant with closed eyes at a specific frequency (1111Hz). During the arithmetic condition, subjects were asked to subtract 5 from 100. If they reached zero or lost track, they had to start again at 100. Figures 2(a) illustrate the five-minute rule for the task, and 2(b) shows the cognitive task protocols.

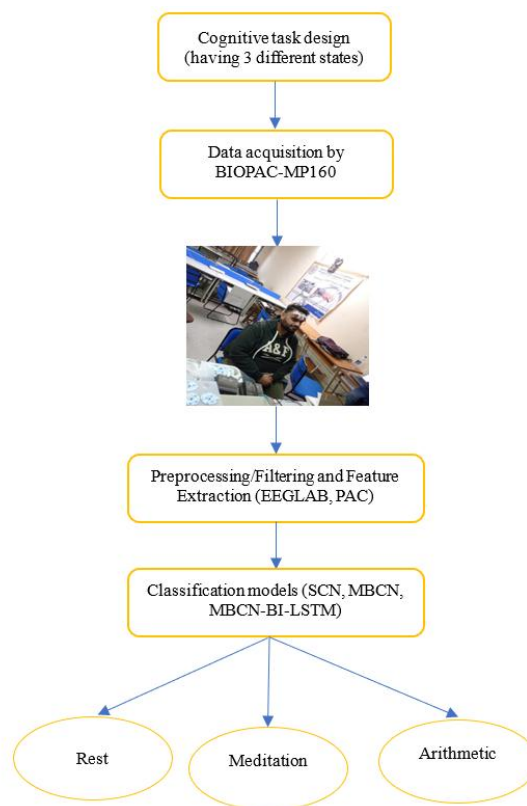
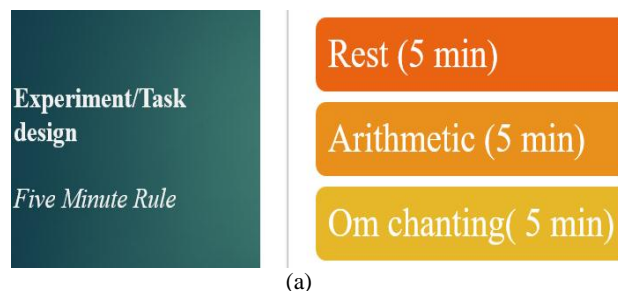


Figure 1 Block description of the proposed methodology





(b)

Figure 2 Illustrates the (a) Five-minute rule; (b) Cognitive task protocols

3.2 Data description

During the data acquisition process, EEG data of twenty-seven subjects ($N=27$, $S.D.=2.18$, $Mean=30.81$, $Variance=4.77$) were collected with a sampling rate of 128 Hz. Out of 27 subjects, 18 were men and 9 were women. Firstly, we have acquired the data of two F1 & F2 channels for three stages (rest, meditation, and arithmetic). Consecutively we have acquired the data of two other positions, i.e., F3, F4 and F7, F8, for three different mental stages. In the rest state for subject one, we have taken data of three positions and one minute allocated for each position. In this way, we have collected three-minute data of the resting stage for subject one. In the same way, we have collected the samples of the other two states, i.e., meditation and arithmetic states. The total number of samples for subject one of nine min was 69120. The demography of the subjects is presented in *Table 1*. BIOPAC MP-160 was used for the EEG acquisition process, and EEG electrodes were located according to the specific task requirements. The data was collected on non-working days (Saturday and Sunday) from 4.00 p.m. IST to 7.00 p.m. IST. The advertisement was published in templates pasted within the university premises for this voluntary data acquisition task. Subjects signed a consent form where they mentioned whether they had any physiological problem or faced it in the past, either taking any medication or suffering from any illness. Nobody was an alcoholic, and one subject was left-handed out of 27 subjects. There was one more parameter, and we investigated this too by asking the person how they felt when they were ready for the data acquisition, anxious, or feeling normal. The data acquisition process was postponed until the particular subject felt normal. The data was collected between November 2020 and January 2021. The electrodes were placed following an internationally recognized

10-20 system, as shown in *Figure 3*. Before attaching the electrodes, the size and shape of the test subject's heads were considered. The head was measured individually by Cadwell tape, and electrodes were placed with the exact measurement of the dimensions of the individual head. Several calculations were carried out with each subject for the results of six different frontal positions.

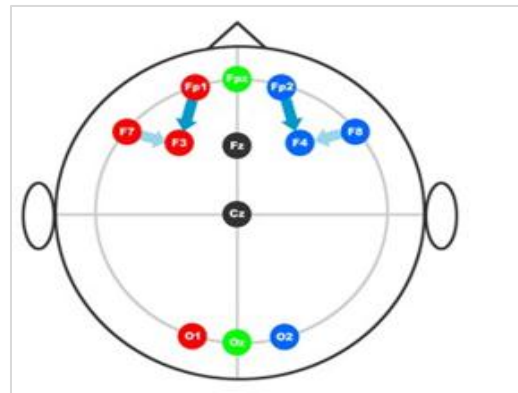


Figure 3 Electrode placements: international 10-20 system (positions Fp1, Fp2, F3, F4, F7, F8)

The placement of the electrodes was rechecked before starting the subsequent measurement. First, the EEG electrodes were placed in Fp1 and Fp2 positions, and the data was recorded for the designed cognitive task. Then the same pattern was repeated with changed electrode positions, i.e., F3, F4, and F7, F8 with Ag/AgCl electrodes. The scalp surfaces were cleaned with a disinfectant to minimize the impedance before attaching the EEG electrodes. Placing the electrodes in different positions was relatively easy (i.e., in most male subjects). Still, in some cases (i.e., female subjects), placing the electrodes was difficult at F3, F4, F7, and F8 positions due to the interference of hairs. All participants were asked to come with a cleansed scalp and hair to reduce excess oil, dandruff, and dirt from the scalp. Therefore, several attempts have been made to extract the data from these positions. The data were collected in the laboratory when no other person/student was present to make the noise and interruptions. The appropriate time was the evening when the laboratory was empty, and the off days were chosen for the same reason. The subjects were asked to be available for this voluntary activity on non-working days. Some test subjects are shown in *Figure 4* during the task.

Table 1 Demography of subjects

No. of subjects	Gender/ Age	Education status	The present state of mind	Alcoholic	Any physiological problem	Any medication
27	31+-4 years 18M,9F	We chose all the graduate subjects. For better results, we decided only on engineering graduates.	Suppose a subject is found depressed or stressed and non-eligible to give data. We tried the next day with that subject.	None	None	One is diabetic type 2, so we exclude him from this data acquisition process.



Figure 4 Different subjects during data acquisition

3.3 Data pre-processing

In this study, a cognitive task has been designed (having three different states). BIOPAC-MP-160 has been used for data acquisition. Then the raw data is pre-processed in the EEGLAB. The primary filtering (0.5 to 40 Hz) has been performed with a second-order Butterworth low-pass filter. Data visualization has also been done to remove unwanted spikes and exogenous artifacts from the data. The artifacts and

noises have been extracted using EEGLAB. Some significant functions of EEGLAB are filtering, artifact removal, re-referencing, resampling, ICA implementation, etc. The data visualization of channels F3 & F4 with respective topographic plots are also shown in *Figure 5*. After the pre-processing, the data was used for PAC for the MI value findings. The mathematical modeling and the various steps are explained in this section.

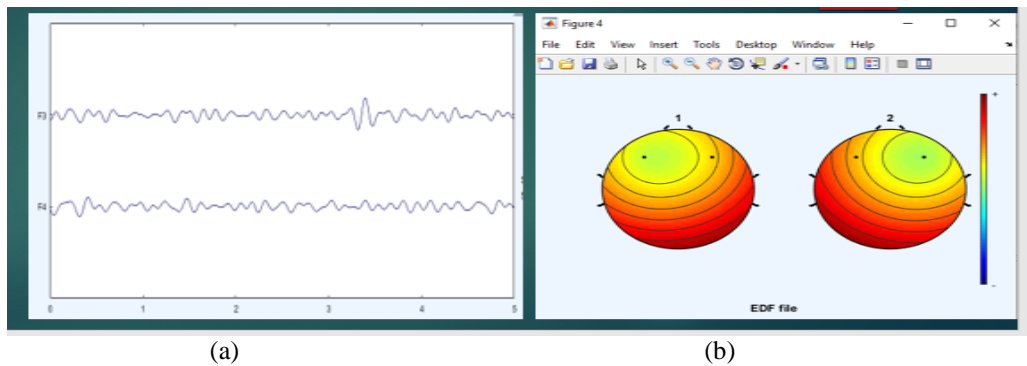


Figure 5 illustrates the (a) Visualization of pre-processed EEG data of channels F3 & F4; (b) Respective topographic maps in a 2-D circular view

3.4 Feature extraction

In this study, the authors have generated discriminative features, i.e., MI values using PAC that reduces the dimensions of the signal and makes it

easy to intercept the patterns corresponding to the different states of the cognitive task. The process flow diagram of MI values finding is illustrated in *Figure 6*. The phase angles of EEG signals have been

estimated by Hilbert transform in lower frequency ranges of alpha and theta bands with a band-pass filter. It provides us several phase-related time series outputs. The amplitudes related to high frequencies have been extracted from the high-frequency EEG ranges using a band-pass filter. It provides us several amplitude-related time series points. The MI values for every electrode have been calculated from these phases and magnitude values applying the Hilbert transform for the different cognitive task states. The MI values are the features that suitably best distinguish the different states of any cognitive/mental task. These extracted MI features for the different cognitive task states were fed as the input to the proposed architectures to differentiate the cognitive task states.

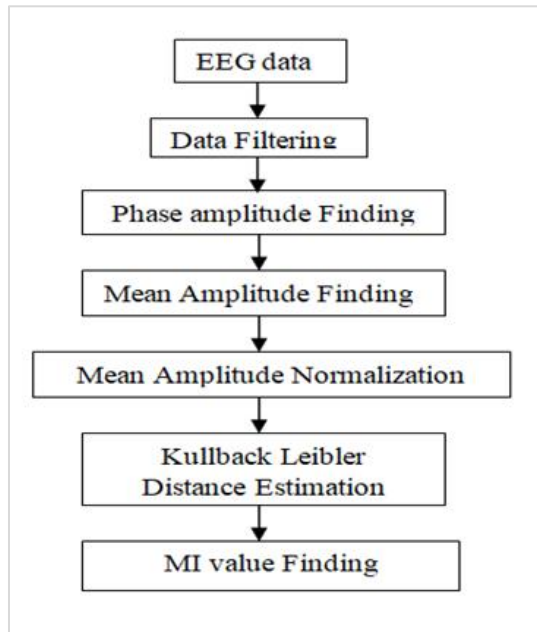


Figure 6 Block diagram of MI value estimation

The following are the stages involved in finding the MI values:

Stage 1. The EEG data extracted from the EEGLAB d(t) is segmented into frequency bands f1 and f2. The filtered signals will be df1(t) and df2(t).

Stage 2. Then, the Hilbert transform is used to extract the phase [Pf1(t)] and the amplitude [Af2(t)] and then created a combined time series [Pf1(t), Af2(t)], which provides the amplitude of f2 oscillation at each segment of f1 pulse.

Stage 3. The phases Pf 1(t) are then segmented. We find the mean amplitude distribution for each phase segment. It shows the mean Af2 value at the phase sector k as Af2Φf1 (k).

Stage 4. Normalization of mean amplitude Af2Pf1 has been calculated by separating the value at each segment by the adding it over all sectors. M is the number of total phase sectors. The amplitude vs. phase plot can be determined to plot X(k) against the phase sector. X(k) can be calculated by Equation 1.

$$X(k) = Af2Pf1(k) / \sum_1^M Af2Pf1 \quad (1)$$

Stage 5. The deviation of amplitude dispersal Z from uniform dispersal denotes the PAC. Kd distance is utilized to quantify this deviation where Kd is the width of Z from a uniform dispersal (Ud) which is associated to Shannon entropy specified by Equation 2.

$$Jkd(Z, Ud) = \log(g) - [\sum_{k=1}^M Z(k) \log[Z(k)]] \quad (2)$$

where, log(g) denotes the greatest possible entropy for uniform distribution and $[\sum_{k=1}^M Z(k) \log[Z(k)]]$ denotes the entropy, so the Kd distance is the deviation between the entropy and the greatest possible entropy.

Stage 6. Ultimately, the MI values have been easily determined using Equations 3 and 4.

$$MI = \frac{\log(g) - [-\sum_{k=1}^g Z(k) \log[Z(k)]]}{\log(g)} \quad (3)$$

$$MI = \frac{Jkd(Z, Ud)}{\log(g)} \quad (4)$$

This MI calculates the difference between the phase-amplitude distribution and the uniformly distributed KL divergence.

3.5 Proposed deep learning architecture

A CNN is a network architecture for deep learning which learns directly from data. CNNs are particularly useful for finding patterns in images to recognize objects. They can also be quite effective for classifying non-image data such as audio, time series, and signal data. Deep learning is a subset of machine learning consisting of algorithms inspired by the human brain's or neural networks' functioning. It has been observed from previous research that CNN is able to capture only short-term dependencies of the temporal sequence of input fixed-length vector. The time series data, which contains a series of points, are not able to infer any particular state; therefore, long-term dependencies are required to retain in deep learning models for the improvement in the recognition task. In this research, we have combined CNN and Bi-LSTM to retain both short- and long-term dependencies. The LSTM networks are proved very successful in case time series sequences for inferring the various states. A classifier model has been proposed to classify the three different states of a designed cognitive task upon receiving a set of featured vectors. The classifier employed and the

extracted features also affect the efficiency of a BCI system [55]. In the previous literature, the EEG signal was given as the CNN input to classify the motor imagery task [56] directly. Before discussing our proposed MBCN-Bi-LSTM model, the authors want to remind the previous methods used in the literature were SCN and MBCN [23]. Typically, a CNN block consists of various layers and activation functions [57]. In our proposed models, there are three branches (i.e., 1,2,3). The different MI values have been created for every subject, test, and electrode position using PAC and given as inputs of branches 1, 2, and 3. The mathematical equation for the generalized Conv1D at depth r with the input $x^{(p)}$ where p ranges from 1 to P is given in Equation 5:

$$C^{(r)}(n) = \sum_p^P \sum_k^K W_C^{(p,r)}(k) x^{(p)}(n+k-1) + b_C^{(r)}(n); \quad 1 \leq n \leq N \quad (5)$$

Where K is the kernel size, $W_C^{(p,r)}$ is the weight matrix and $b_C^{(r)}$ is the bias vector, the total number of feature maps for the input layer is symbolized as P , and N is the output length. The network parameters in the Conv1D layer are learned via backpropagation to reduce the classification error. The authors designed architecture with a one-dimensional (1D) CNN, batch normalization layer, and activation function named rectified linear unit (ReLU) and these blocks are stacked. The SoftMax activation function was used in the end. The SCN model used in the previous paper has two main blocks convolution and a fully connected block. The output of the convolution block, which contains various layers and activation functions, is provided to the input of a fully connected dense layer. The CNN block has several layers: batch normalization, dense, max pooling, and activation. Typically, it can be seen that if we increase the length of CNN architecture, the accuracy is also enhanced, but the computation cost also increases. The authors proposed a recurrent networks-based deep learning architecture that converts and mixes the input at different levels, with three Convolution layers connected parallel. This technique provides feature findings in various time segments. The next MBCN model has two essential architectures: LSTM and CNN architecture. The Dropout and Global average pooling values have been included to remove the complexity and overfitting. The block description of the proposed MBCN-Bi-LSTM model classifier is demonstrated in Figure 7. This model consists of three heads, each having similar inputs extracted from the different states of the cognitive task. Each head has a Conv1D layer and 128, 64, and 32 filters, respectively.

Based on the extracted features of different scales of different temporal locations, the size of the filters for head-1, head-2, and head-3 are 3, 5, and 7, respectively. The input vector is provided to Conv1D, and the ReLU activation function is used. The input is followed by three different branches with a filter size of 3, 5, and 7 in Head-1, Head-2, and Head-3, respectively. A dropout layer with a drop factor of 0.3 follows the second Conv1D layer. The dropout layer is used to overcome the overfitting issues. Dropout is a method in which the arbitrarily chosen neurons are neglected during training, i.e., their participation in the activation of downward neurons is temporarily extracted on the propulsive parts, and anywhere changes are not applied to the neurons on the previous pass. Next comes a max-pooling 1D layer with pool size=2. Maximum pooling is performed to condense the dimensions of the feature maps.

The generalized Equations for max-pooling and ReLU activation function are presented in Equation 6 to Equation 8.

$$MP^{(r)}(n) = \text{Max} \left(Y^{(r)}(2n-1), Y^{(r)}(n) \right) \quad (6)$$

Where Y is the output from the previous layer

$$R_{MP}^{(r)}(n) = \text{ReLU} \left(MP^{(r)}(n) \right) = \text{Max} \left(0, MP^{(r)}(n) \right) \quad (7)$$

$$R_C^{(r)}(n) = \text{ReLU} \left(C^{(r)}(n) \right) = \text{Max} \left(0, C^{(r)}(n) \right) \quad (8)$$

Three branches of the proposed method provided three outputs; therefore, before delivering it to the LSTM layer, we concatenate the three outputs to convert them as a single input vector.

Concatenation (branch_1 o/p, branch_2 o/p, branch_3 o/p)

An LSTM model generally consists of three gates: forget, input, and output.

(1): Forget Gate. A sigmoid function (σ) is usually used for this gate to decide what information needs to be removed from the LSTM memory. The output of the forget gate is represented in Equation 9.

$$f_t = \sigma(W_{fh}h_t + W_{fx}x_t + b_f) \quad (9)$$

X_t is the input at time t , h_t is the cell state, and W and b denote the weight and bias, respectively.

(2): Input Gate. This gate decides whether or not the new information may be added to the LSTM memory. This gate contains two layers, i.e., a sigmoidal (σ) layer that decides the value that has

been updated. The second layer, i.e., the "tanh" layer, creates the vectors for new values that may be added to the LSTM. The output of these two layers is represented in Equations 10 and 11.

$$i_t = \sigma(W_{ih}h_t + W_{ix}x_t + b_i) \tag{10}$$

$$dc_t = \tanh(W_{ch}h_{t-1} + W_{cx}x_t + b_c) \tag{11}$$

Where ct indicates the vector of new values, combining these two layers provides an update to the LSTM memory. Here the current value is forgotten using the forget gate layer by multiplying the old value (i.e., $ct-1$) followed by adding the new candidate value $it * c_t$. Equation 12 represents its mathematical equivalence:

$$c_t = f_t \circ c_{t-1} + i_t \circ dc_t \tag{12}$$

Where ft is the result of the forget gate.

(3): Output Gate. This gate uses a sigmoid layer (σ) to judge which part of the LSTM memory contributes to the output. Then, it performs a non-linear \tanh function to lie these values within -1 and 1 . Lastly, the result is multiplied by the output of a sigmoid layer. The following Equations 13 and 14 represent the formulas to compute the output:

$$o_t = \sigma(W_{oh}h_t + W_{ox}x_t + b_o) \tag{13}$$

$$h_t = o_t \circ \tanh(c_t) \tag{14}$$

Where ot is the output value, and ht is its representation as a value between -1 and 1 .

The Bi-LSTMs is an extension of the described LSTM models in which two LSTMs are applied to the input data. In the first round, an LSTM is applied

on the input sequence (i.e., forward layer). In the second round, the reverse form of the input sequence is fed into the LSTM model (i.e., backward layer). Applying the LSTM twice leads to improving long-term learning dependencies and, thus, consequently, will enhance the accuracy of the model [58]. Two Bi-LSTM layers are used in the architecture to improve the model performance. The first Bi-LSTM layers contain 64 units that are fed into the next Bi-LSTM layer having 128 units. The next is a batch normalization layer which accelerates the training and provides some regulation by maintaining the epochs and reducing generalization errors. It preserves data flow and then categorizes the input using the softmax enable function at the output layer. The activation function determines a neuron's activity status. It will use a basic mathematical operation to determine whether the neuron's input to the network is necessary throughout the reduction process. Table 2 consists the hyper parameters of the proposed model.

Table 2 Hyper-parameters

S. No.	Parameter	Values
1	Optimizer	Adam
2	Loss	Categorical cross-entropy
3	Epochs	500
4	Learning rate	0.0001
5	Batch size	400
6	Metrics	Accuracy

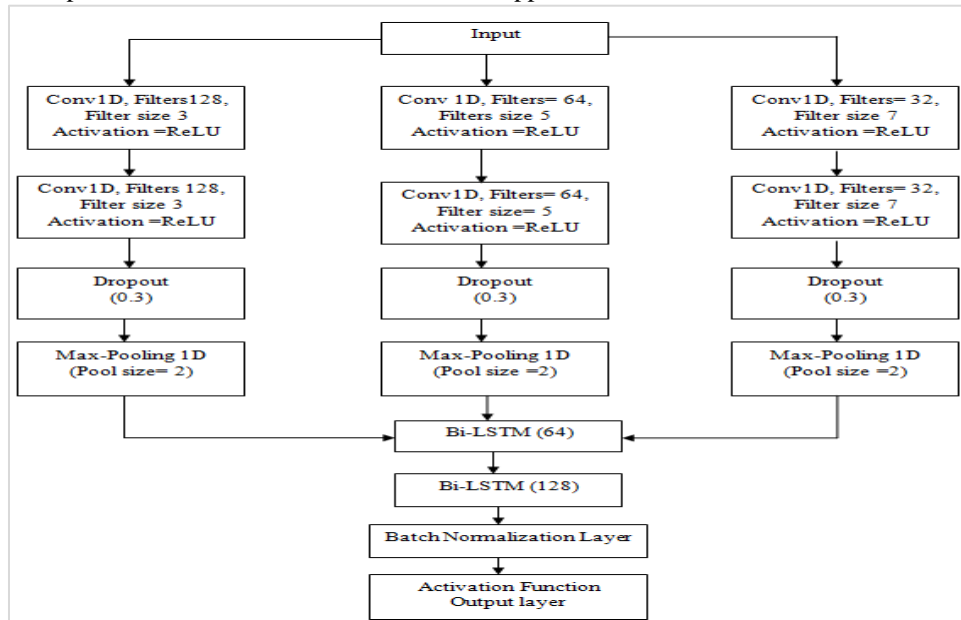


Figure 7 Block description of the proposed model

4.Result

EEG signals were recorded from different subjects with their written consent using BIOPAC-MP-160 in a real environment for further processing. A total of 7860 samples were extracted from a one-minute data sample of EEG. In the SCN model from 2510 samples at-rest state, 2280 were predicted true, i.e.90.84%. The performance indicators included in this study are the F1-score, recall, precision, accuracy, and confusion matrix. We may infer the fundamental definitions of recall, precision, and accuracy from the literature; for example, accuracy is defined as the proportion of adequately classified samples to all accessible samples. When the activities are correctly classified, they are noted as true positives (TP) and true negatives (TN); however, incorrect classification results in false negatives (FN) and false positives (FP). These parameters can be used to define the performance measures, including accuracy, precision, recall, and F1 score from the following Equation 15 to Equation 18.

$$Accuracy = \frac{TP+TN}{TP+TN+FP+FN} \quad (15)$$

The ratio of all the positive predicted samples correctly to the total number of samples available is defined as the precision.

$$Precision = \frac{TP}{TP+FP} \quad (16)$$

The ratio of positives predicted correctly to the actual number of positive samples is known as recall.

$$Recall = \frac{TP}{TP+FN} \quad (17)$$

The mean of the recall and precision is known as F1-score.

$$F_1 - Score = \frac{2 \times Precision \times Recall}{Precision + Recall} \quad (18)$$

The entire misclassification rate is displayed in the confusion matrix. The columns indicate the erroneous labels the classifier predicted, and the rows reflect the genuine ones. It provides the classification performance of the model. *Table 3, 4, and 5* shows the confusion matrix for the cognitive task classification having three different states, i.e., rest, meditation, and arithmetic.

The accuracy, precision, recall, and F1 scores were obtained from the designed cognitive task EEG

dataset. While in the previous literature, the methods provided the comparisons of different techniques in terms of accuracy only and significantly fewer descriptions of the precision, recall, or F1-score are available. The EEG dataset acquisition is a crucial step in minimizing the overlapping of frequency components. Subjects sat relaxed with their eyes closed without clenching their jaws with eyes closed to reduce artifacts. Our proposed approach is validated by taking 30 % of the total data points as the testing set and 70% as the training set.

Table 3 Confusion matrix for SCN (Accuracy 88.94)

Actual \ Predicted	Rest	Meditation	Arithmetic
Rest	2280	110	120
Meditation	204	2776	280
Arithmetic	52	80	2278

Table 4 Confusion matrix for MBCN (Accuracy 91.01)

Actual \ Predicted	Rest	Meditation	Arithmetic
Rest	2200	150	160
Meditation	160	2400	200
Arithmetic	50	60	2300

Table 5 Confusion matrix for MBCN-Bi-LSTM (Accuracy 97.99)

Actual \ Predicted	Rest	Meditation	Arithmetic
Rest	2508	2	0
Meditation	69	2601	90
Arithmetic	1	1	2408

The models were trained on a laptop running Windows 10 64-bit, an Intel Core i5 processor clocked at 2.2 GHz, and 4 GB of RAM. Five hundred epochs of the data set, with a 64-batch training size, were divided into 70:30 training and validation portions. The training and validation accuracy plots for SCN, MBCN, and MBCN-Bi-LSTM obtained for the cognitive task EEG dataset are displayed in *Figures 8, 9, and 10*. We can say that the results for MBCN-Bi-LSTM have greater accuracy than both SCN and MBCN models, and these models can classify the cognitive task states effectively. *Table 6* shows the cognitive test's precision, recall, and F1-score states of these different models. The proposed model provides higher accuracy than others. *Figure 11* expresses the bar graph of precision, recall, and F1 score in the three different states of the cognitive task, i.e., rest, meditation, and arithmetic.

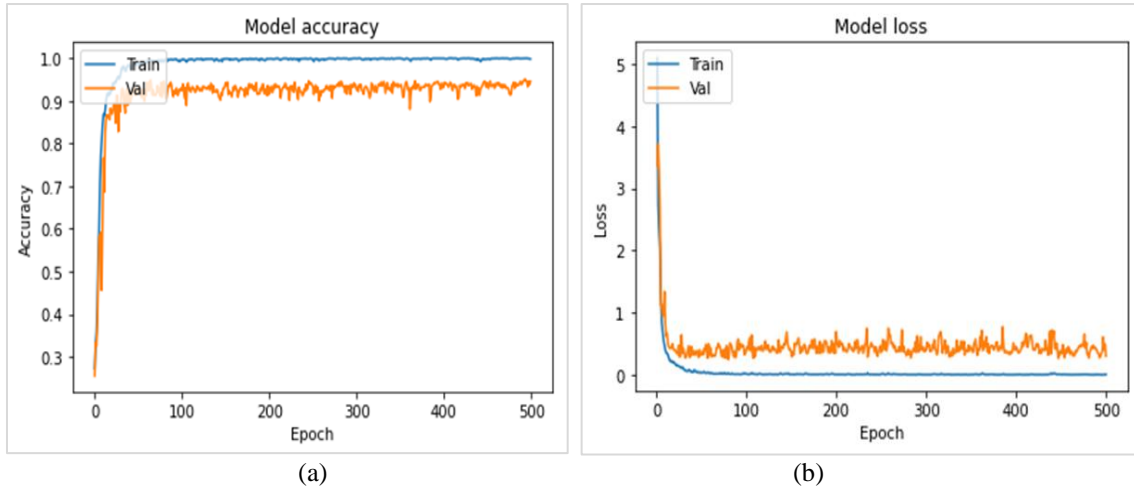


Figure 8 (a, b) Accuracy and model loss curves for SCN

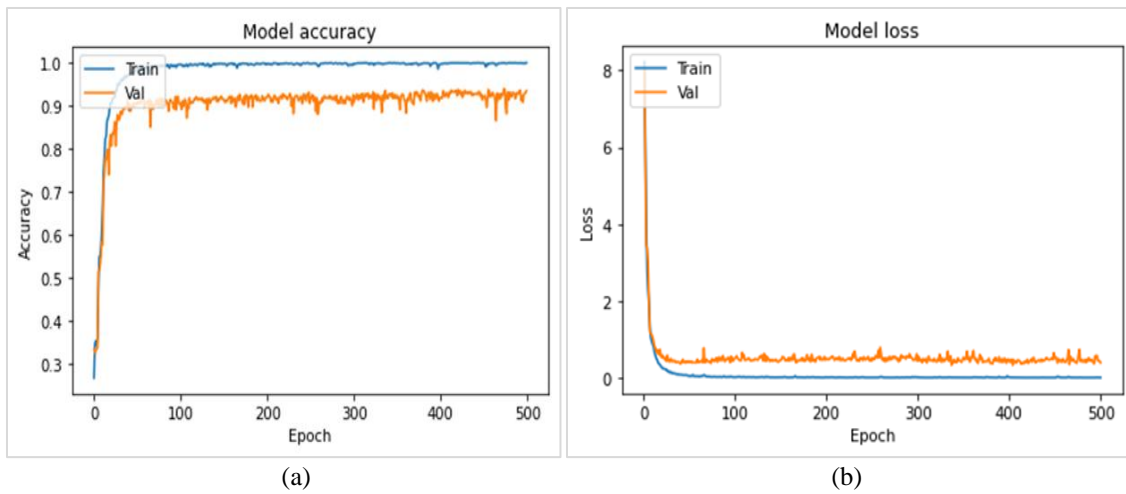


Figure 9 (a, b) Accuracy and model loss curves for MBCN

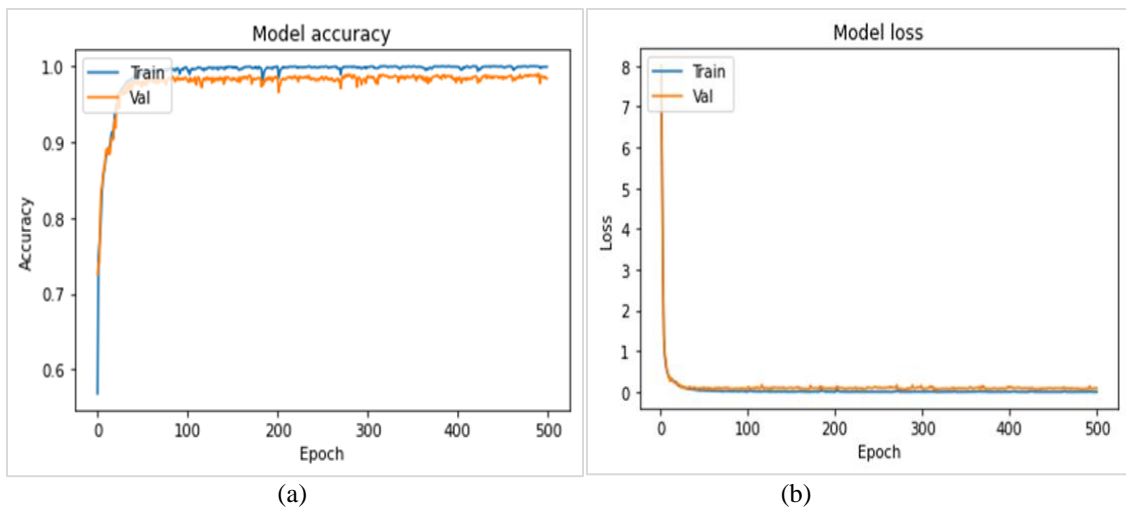
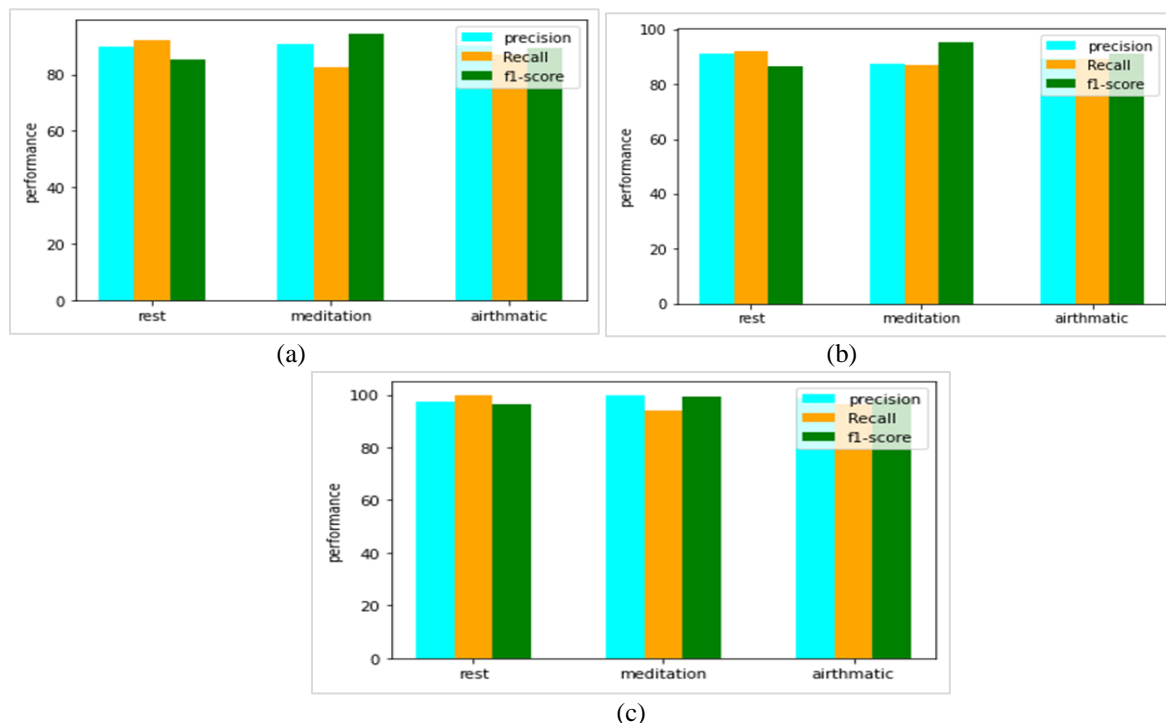


Figure 10 (a, b) Accuracy and model loss curves for MBCN-Bi-LSTM

Table 6 Classification results: SCN, MBCN, MBCN-Bi-LSTM

Cognitive state	SCN model			MBCN model			MBCN-bi-LSTM model		
	Precision	Recall	F1-Score	Precision	Recall	F1-Score	Precision	Recall	F1-Score
Rest	89.90	90.83	90.35	91.28	87.64	89.41	97.28	99.92	98.58
Meditation	92.29	82.46	87.09	91.95	86.95	89.37	99.88	94.23	96.17
Arithmetic	85.00	94.52	89.53	86.46	95.43	91.22	96.39	99.91	98.11

**Figure 11** Bar graph of precision, recall, and F1 score for different stages of the brain (a) Model SCN, (b) Model MBCN, (c) Model MBCN-Bi-LSTM

5. Discussion

Various standard features such as spectral analysis, PSD, Event-related potentials (ERPs), powers in different frequency bands, and alpha band relationships were extracted during the tasks by Hu and Zhang [59]. The early detection of Alzheimer disease (AD) by mild cognitive impairment (MCI) has been proposed by Fouladi et al. [60]. The authors proposed two different deep learning architectures for the classification of subjects into AD, MCI, and healthy control using 19-channel scalp EEG data. Modified CCN found an average accuracy of 92%. Various research articles have presented the classification of EEG signals associated with a mental task. In contrast, the deep neural network (DNN) classifier has been used to classify the EEG-based mental task classification, and the accuracy achieved 77.62% [61]. PAC was utilized for feature extraction purposes. In the case of machine learning approaches, the user must have to reduce the signal in its features, and then a suitable classifier is used to

classify these features. In deep learning methods, the classifier can automatically detect the features. A CNN performs better than the older conventional methods for better learning and classification accuracy. A multiscale high-density convolutional neural network (MHCNN) has been proposed to classify EEG task states (before and after cognitive training), and the classification results were compared with CNN. The results show that MHCNN outperforms with an accuracy of 98% [62]. A CNN-based automatic sleep stage detection has been done by Cui et al. [63]. The previous literature used conventional feature extraction methods and classification techniques but utilized automatic sleep stage prediction. An average accuracy of 92.2% has been achieved in the classification of five stages of sleep using the online available sleep dataset from the Institute of System and Robotics, University of Coimbra (ISRUC). The automatic features were extracted in 30 seconds. A cascaded recurrent neural network-based-LSTM network has been used to

assess neurocognitive performance [64]. The average achieved accuracy was 86.7, with an error rate of 13.3. An improved neural network (INN)-based EEG signal classification has been performed by Nagbhusanam et al. [65]. Two layers of LSTM and a four-layer improved CNN algorithm has been proposed to classify the signal. An average accuracy of 78.92 has been achieved by this method. The EEG dataset of Temple University for the normal and abnormal mental conditions has been used to classify these two mental conditions. They used 1D CNN for classification purposes. The study error rate was found 20.06, which is relatively lower than the previous studies. Alcoholism is another state of the brain that affects the person's cognition. Farsi et al. [47] proposed a method to classify the EEG data of the alcoholic and non-alcoholic states of the brain. Two deep learning-based approaches have been used to classify the EEG signals. In one of the approaches, the authors extracted features of the signal using the PAC method, and then the extracted features were used as the input to the CNN. In the second approach, the raw EEG data are directly used as the input to the LSTM-based classifier. They found that better classification was achieved when the raw data was directly applied to the deep classifier. Dvorak et al. [66] classified cognitive behavior from the EEG signal. Eight different cognitive tasks have been performed. Three different methods, i.e., power analysis, phase locking value estimation, and PAC, have been used to classify these tasks. The authors found that the PAC has the second maximum classification accuracy of 78.8%. In contrast, when

all three measures were combined, the dataset obtained an overall prediction accuracy of 82.3%. Yildirim et al. [67] proposed a deep 1D CNN model for the classification of normal and abnormal mental states using EEG signals. Different mental states, i.e., focused, unfocused, and drowsiness, have been classified by Aci et al. [68]. Different approaches like SVM, K-nearest neighbour (KNN), and neuro-fuzzy have been utilized for classification purposes, and the authors found the maximum accuracy with the SVM classifier of 96.70%. Toa et al. [69] proposed a method to detect the attention level, i.e., whether the subject is attentive or inattentive. The proposed convolution attention memory network (CAMNN) model outperforms to the previously used method with an accuracy of 92%. Mohanavelu et al. [70] used different machine learning approaches to identify the mental workload of the flight pilots during different phases of flight, i.e., takeoff, landing, etc. Using EEG features, the cognitive workload was classified, and the LDA performed better than the other two methods. The SCN and MBCN models have been proposed in [23]. The authors applied these SCN and LSTM models in the acquired EEG dataset, getting an accuracy of 88.94% and 91.01%, respectively. At the same time, our proposed MBCN-Bi-LSTM model gives us an accuracy of 97.99 %. This MBCN-Bi-LSTM architecture has various convolutional layers, and the feature map length has been reduced at each layer more accurately. The Accuracy and classification techniques have been compared in *Table 7*.

Table 7 Comparison of performance with different methods for cognitive task classification

Approach	References	Classification accuracy	Cognitive /mental state	Error rate
CNN	Fouladi et al. [60]	92.00	AD detection by cognitive task	8.00
DNN	Siddiqui et al. [61]	77.62	Mental task	22.38
MHCNN	Wen et al. [62]	98.00	Cognitive task	2.0
RNN plus LSTM	Cui et al. [63]	92.2	Different sleep stages	7.8
CNN	Michielli et al. [64]	86.7	Cognitive/mental capacity assessment	13.3
INN	Nagabhusanam et al.[65]	78.92	Mild cognitive task	21.08
LSTM	Forsi et al.[47]	93.00	Alcoholic, non-alcoholic	7.00
ML	Dvorak et al.[66]	82.3	8 cognitive tasks	17.7
CNN	Yildirim et al. [67]	79.94	Normal, abnormal	20.06
ML	Aci et al.[68]	97.87	Rest, focused, unfocused, drowsiness	2.13
CAMNN	Toa et al. [69]	92.00	Attentive, inattentive	18.00
LDA	Mohanavelu et al. [70]	72.44	Cognitive workload	27.56
MBCN, SCN	Sucheta et al. [23]	88.33	4 cognitive tasks	11.67
SCN	This Study	88.94	Rest, meditation,	11.06
MBCN		91.09	Arithmetic	8.91
MBCN-Bi-LSTM		97.99		2.01

We have achieved better classification accuracy from our proposed model than in the previous literature. We have three states of mental condition and achieved accuracies of 88.94, 91.09, and 97.99. The error rate is relatively low than the previous methods.

5.1 Different feature combinations of the proposed model

Table 8 shows the various possible combinations of the proposed architecture. In model A, Branch 1 has 64 filters, filter size 5, activation function ReLU, and dropout is 0.4%. Branch 2 has 32 filters with filter size 5, activation function ReLU and drop out of 0.4%. In the third branch of model A, we used 128 filters with size 3. In the convolution layer, the activation function is ReLU and has a dropout of

0.4%. The average accuracy of model A is 95.07. In the same manner, Model B contains three branches. The first branch has 32 filters with filter size 3 having ReLU activation function with a dropout of 0.5%. The second branch has 128 filters with filter size five and a ReLU activation function with a dropout of 0.5%. The third branch has 64 filters, and three branches have activation function ReLU and dropout of 0.5%. The overall average accuracy of Model B has been seen as 95.80. Similarly, in model C and the proposed one, the filter size, no. of layers, activation function used, and dropout % are shown in Table 8. Our proposed model has relatively better classification accuracy, i.e., 97.99, than the other possible combinations.

Table 8 Different possible combinations of the proposed architecture

	Filter	Filter size	Layer	Activation	Dropout%	Branch no	Accuracy
Model A	64	5	convolution	ReLU	0.4	1	95.07
	32	7	convolution	ReLU	0.4	2	
	128	3	convolution	ReLU	0.4	3	
Model B	32	3	convolution	ReLU	0.5	1	95.80
	128	5	convolution	ReLU	0.5	2	
	64	3	convolution	ReLU	0.5	3	
Model C	32	3	convolution	ReLU	0.3	1	96.02
	128	5	convolution	ReLU	0.3	2	
	64	7	convolution	ReLU	0.3	3	
Model D	16	3	convolution	ReLU	0.5	1	96.69
	64	7	convolution	ReLU	0.7	2	
	32	3	convolution	ReLU	0.5	3	
Proposed	128	3	convolution	ReLU	0.3	1	97.99
	64	5	convolution	ReLU	0.3	2	
	32	7	convolution	ReLU	0.3	3	

5.2 Study limitations

The proposed MBCN-Bi-LSTM model is complex, so the system complexity has to be reduced in the future. Due to its complex structure, the computational burden is also high. That's why a less complex system with fewer layers must be developed to overcome this issue. The proposed model has been used only on the EEG dataset. More physiological datasets, such as EMG and ECG with different conditions, are also implemented in our proposed model, and the results can be compared with existing research. One of the important factors during the classification stage is the number of states. Our acquired dataset has three stages, i.e., rest, meditation, and arithmetic. More the number of states may directly affect the system's accuracy. A dataset with more classes can be classified with the proposed model. The available online datasets may provide better accuracy with the proposed model. The number of participants is also important for any

cognitive/ mental state classification. But ethical concerns make it difficult to prepare the participants for the study/experimentation. In the present study, we have 27 participants, but this number can be increased to 50-100 participants to make the proposed system more reliable. A complete list of abbreviations is shown in *Appendix I*.

6. Conclusion and future work

In this paper, MI values were measured by PAC performed on dataset EEG. The authors developed an MBCN-Bi-LSTM and compared its classification results with the previous techniques to classify given EEG signals for the cognitive task. The MI values have been used as features for the different states of the task, and these MI values have been associated with the amplitude and phase components of the different states of the dataset. Data acquisition is complex, i.e., accurately performing the different test states simultaneously with the subject. In future

work, one can increase the cognitive task state and perform these techniques on these states. For real-world applications, one can use this classification method when some people are performing meditation/rest/arithmetic or some different state means to say whether the person is immersed in the state or not. The dataset can be taken by various wireless instruments and performed in a real-time application. The whole scalp can be included in further research as we focus on the frontal lobe. The possibilities of more detailed research in this area are available.

Acknowledgment

The authors would like to thank Dr Jaspreet Singh from the Department of Electrical and Instrumentation Engineering at Sant Longowal Institute of Engineering and Technology for their insightful comments and suggestions to make the manuscript more comprehensible.

Conflicts of interest

The authors have no conflicts of interest to declare.

Author's contributions statement

Hitesh Yadav: Conceptualization, study design: cognitive task design, data collection: using BIOPAC MP-160, analysis and interpretation of results: on EEGLAB and python, writing-original draft. **Surita Maini:** Supervision, study investigation, investigation on challenges, analysis and interpretation of results, writing- editing and reviewing the article.

References

- [1] Vansteensel MJ, Pels EG, Bleichner MG, Branco MP, Denison T, Freudenburg ZV et al. Fully implanted brain-computer interface in a locked-in patient with ALS. *New England Journal of Medicine*. 2016; 375(21):2060-6.
- [2] Wang H, Chang W, Zhang C. Functional brain network and multichannel analysis for the P300-based brain computer interface system of lying detection. *Expert Systems with Applications*. 2016; 53:117-28.
- [3] Fujiwara K, Abe E, Kamata K, Nakayama C, Suzuki Y, Yamakawa T, et al. Heart rate variability-based driver drowsiness detection and its validation with EEG. *IEEE Transactions on Biomedical Engineering*. 2018; 66(6):1769-78.
- [4] Gao X, Wang Y, Chen X, Gao S. Interface, interaction, and intelligence in generalized brain-computer interfaces. *Trends in Cognitive Sciences*. 2021; 25(8):671-84.
- [5] Hramov AE, Maksimenko VA, Pisarchik AN. Physical principles of brain-computer interfaces and their applications for rehabilitation, robotics and control of human brain states. *Physics Reports*. 2021; 918:1-33.
- [6] Yadav D, Yadav S, Veer K. A comprehensive assessment of brain computer interfaces: recent trends and challenges. *Journal of Neuroscience Methods*. 2020; 346(2020):1-20.
- [7] Gu X, Cao Z, Jolfaei A, Xu P, Wu D, Jung TP, et al. EEG-based brain-computer interfaces (BCIs): A survey of recent studies on signal sensing technologies and computational intelligence approaches and their applications. *IEEE/ACM Transactions on Computational Biology and Bioinformatics*. 2021; 18(5):1645-66.
- [8] Bagheri M, Power SD. Simultaneous classification of both mental workload and stress level suitable for an online passive brain-computer interface. *Sensors*. 2022; 22(2):1-17.
- [9] Lohani M, Payne BR, Strayer DL. A review of psychophysiological measures to assess cognitive states in real-world driving. *Frontiers in Human Neuroscience*. 2019; 13:1-27.
- [10] Kongwudhikunakorn S, Kiatthaveephong S, Thanontip K, Leelaarporn P, Piriyajitakonkij M, Charoenpattarawat T, et al. A pilot study on visually stimulated cognitive tasks for EEG-based dementia recognition. *IEEE Transactions on Instrumentation and Measurement*. 2021; 70:1-10.
- [11] Sharma S, Singh G, Sharma M. A comprehensive review and analysis of supervised-learning and soft computing techniques for stress diagnosis in humans. *Computers in Biology and Medicine*. 2021; 134(2021):1-19.
- [12] Keil A, Bernat EM, Cohen MX, Ding M, Fabiani M, Gratton G, et al. Recommendations and publication guidelines for studies using frequency domain and time-frequency domain analyses of neural time series. *Psychophysiology*. 2022; 59(5):1-37.
- [13] Nafea MS, Ismail ZH. Supervised machine learning and deep learning techniques for epileptic seizure recognition using EEG signals-a systematic literature review. *Bioengineering*. 2022; 9(12):1-35.
- [14] Wang J, Wang M. Review of the emotional feature extraction and classification using EEG signals. *Cognitive Robotics*. 2021; 1:29-40.
- [15] Zhou Y, Xu Z, Niu Y, Wang P, Wen X, Wu X, et al. Cross-task cognitive workload recognition based on EEG and domain adaptation. *IEEE Transactions on Neural Systems and Rehabilitation Engineering*. 2022; 30:50-60.
- [16] Zheng X, Chen W, You Y, Jiang Y, Li M, Zhang T. Ensemble deep learning for automated visual classification using EEG signals. *Pattern Recognition*. 2020; 102:1-33.
- [17] Li G, Lee CH, Jung JJ, Youn YC, Camacho D. Deep learning for EEG data analytics: a survey. *Concurrency and Computation: Practice and Experience*. 2020; 32(18):1-13.
- [18] Zhao X, Zhang H, Zhu G, You F, Kuang S, Sun L. A multi-branch 3D convolutional neural network for EEG-based motor imagery classification. *IEEE Transactions on Neural Systems and Rehabilitation Engineering*. 2019; 27(10):2164-77.
- [19] Qiao W, Bi X. Ternary-task convolutional bidirectional neural Turing machine for assessment of

- EEG-based cognitive workload. *Biomedical Signal Processing and Control*. 2020; 57:1-13.
- [20] Abbasi SF, Ahmad J, Tahir A, Awais M, Chen C, Irfan M, et al. EEG-based neonatal sleep-wake classification using multilayer perceptron neural network. *IEEE Access*. 2020; 8:183025-34.
- [21] Ha KW, Jeong JW. Motor imagery EEG classification using capsule networks. *Sensors*. 2019; 19(13):1-20.
- [22] Saccá V, Campolo M, Mirarchi D, Gambardella A, Veltri P, Morabito FC. On the classification of EEG signal by using an SVM based algorithm. *Multidisciplinary Approaches to Neural Computing*. 2018:271-8.
- [23] Suchetha M, Madhumitha R, Sruthi R. Sequential convolutional neural networks for classification of cognitive tasks from EEG signals. *Applied Soft Computing*. 2021; 111(2021):1-14.
- [24] Al-fahoum AS, Al-fraihat AA. Methods of EEG signal features extraction using linear analysis in frequency and time-frequency domains. *International Scholarly Research Notices*. 2014; 2014:1-8.
- [25] Scally B, Burke MR, Bunce D, Delvenne JF. Resting-state EEG power and connectivity are associated with alpha peak frequency slowing in healthy aging. *Neurobiology of Aging*. 2018; 71:149-55.
- [26] Jacobs D, Hilton T, Del CM, Carlen PL, Bardakjian BL. Classification of pre-clinical seizure states using scalp EEG cross-frequency coupling features. *IEEE Transactions on Biomedical Engineering*. 2018; 65(11):2440-9.
- [27] Nuamah JK, Seong Y. Support vector machine (SVM) classification of cognitive tasks based on electroencephalography (EEG) engagement index. *Brain-Computer Interfaces*. 2018; 5(1):1-12.
- [28] Dutta S, Singh M, Kumar A. Automated classification of non-motor mental task in electroencephalogram based brain-computer interface using multivariate autoregressive model in the intrinsic mode function domain. *Biomedical Signal Processing and Control*. 2018; 43:174-82.
- [29] Noshadi S, Abootalebi V, Sadeghi MT, Shahvazian MS. Selection of an efficient feature space for EEG-based mental task discrimination. *Biocybernetics and Biomedical Engineering*. 2014; 34(3):159-68.
- [30] Gupta A, Agrawal RK, Kirar JS, Andreu-perez J, Ding WP, Lin CT, et al. On the utility of power spectral techniques with feature selection techniques for effective mental task classification in noninvasive BCI. *IEEE Transactions on Systems, Man, and Cybernetics: Systems*. 2019; 51(5):3080-92.
- [31] Gaurav AR, Kumar V. EEG-metric based mental stress detection. *Network Biology*. 2018; 8(1):25-34.
- [32] Qayyum A, Khan MA, Mazher M, Suresh M. Classification of EEG learning and resting states using 1d-convolutional neural network for cognitive load assessment. In *student conference on research and development (SCOReD) 2018* (pp. 1-5). IEEE.
- [33] Zhang P, Wang X, Zhang W, Chen J. Learning spatial-spectral-temporal EEG features with recurrent 3D convolutional neural networks for cross-task mental workload assessment. *IEEE Transactions on Neural Systems and Rehabilitation Engineering*. 2018; 27(1):31-42.
- [34] Jiménez-guarneros M, Gómez-gil P. Custom domain adaptation: a new method for cross-subject, EEG-based cognitive load recognition. *IEEE Signal Processing Letters*. 2020; 27:750-4.
- [35] Idowu OP, Ilesanmi AE, Li X, Samuel OW, Fang P, Li G. An integrated deep learning model for motor intention recognition of multi-class EEG signals in upper limb amputees. *Computer Methods and Programs in Biomedicine*. 2021; 206:1-39.
- [36] Liu Q, Cai J, Fan SZ, Abbod MF, Shieh JS, Kung Y, et al. Spectrum analysis of EEG signals using CNN to model patient's consciousness level based on anesthesiologists' experience. *IEEE Access*. 2019; 7:53731-42.
- [37] Schirrmester RT, Springenberg JT, Fiederer LD, Glasstetter M, Eggenberger K, Tangermann M, et al. Deep learning with convolutional neural networks for EEG decoding and visualization. *Human Brain Mapping*. 2017; 38(11):5391-420.
- [38] Lawhern VJ, Solon AJ, Waytowich NR, Gordon SM, Hung CP, Lance BJ. EEGNet: a compact convolutional neural network for EEG-based brain-computer interfaces. *Journal of Neural Engineering*. 2018; 15(5):1-30.
- [39] Yang Y, Wu Q, Qiu M, Wang Y, Chen X. Emotion recognition from multi-channel EEG through parallel convolutional recurrent neural network. In *international joint conference on neural networks 2018* (pp. 1-7). IEEE.
- [40] Bird JJ, Kobylarz J, Faria DR, Ekárt A, Ribeiro EP. Cross-domain MLP and CNN transfer learning for biological signal processing: EEG and EMG. *IEEE Access*. 2020; 8:54789-801.
- [41] Samanta K, Chatterjee S, Bose R. Cross-subject motor imagery tasks EEG signal classification employing multiplex weighted visibility graph and deep feature extraction. *IEEE Sensors Letters*. 2019; 4(1):1-4.
- [42] Kwon S. CLSTM: deep feature-based speech emotion recognition using the hierarchical ConvLSTM network. *Mathematics*. 2020; 8(12):1-19.
- [43] Sajjad M, Kwon S. Clustering-based speech emotion recognition by incorporating learned features and deep BiLSTM. *IEEE Access*. 2020; 8:79861-75.
- [44] Roy Y, Banville H, Albuquerque I, Gramfort A, Falk TH, Faubert J. Deep learning-based electroencephalography analysis: a systematic review. *Journal of Neural Engineering*. 2019; 16(5):1-38.
- [45] Amin SU, Alsulaiman M, Muhammad G, Mekhtiche MA, Hossain MS. Deep learning for EEG motor imagery classification based on multi-layer CNNs feature fusion. *Future Generation Computer Systems*. 2019; 101:542-54.
- [46] Altuwaijri GA, Muhammad G. A multibranch of convolutional neural network models for electroencephalogram-based motor imagery classification. *Biosensors*. 2022; 12(1):1-21.

- [47] Farsi L, Siuly S, Kabir E, Wang H. Classification of alcoholic EEG signals using a deep learning method. *IEEE Sensors Journal*. 2020; 21(3):3552-60.
- [48] Ambrosini E, Vallesi A. Asymmetry in prefrontal resting-state EEG spectral power underlies individual differences in phasic and sustained cognitive control. *Neuroimage*. 2016; 124:843-57.
- [49] Gong R, Wegscheider M, Mühlberg C, Gast R, Fricke C, Rumpf JJ, et al. Spatiotemporal features of β - γ phase-amplitude coupling in Parkinson's disease derived from scalp EEG. *Brain*. 2021; 144(2):487-503.
- [50] Jurkiewicz GJ, Hunt MJ, Żygierewicz J. Addressing pitfalls in phase-amplitude coupling analysis with an extended modulation index toolbox. *Neuroinformatics*. 2021; 19:319-45.
- [51] Tort AB, Komorowski R, Eichenbaum H, Kopell N. Measuring phase-amplitude coupling between neuronal oscillations of different frequencies. *Journal of Neurophysiology*. 2010; 104(2):1195-210.
- [52] Hülsemann MJ, Naumann E, Rasch B. Quantification of phase-amplitude coupling in neuronal oscillations: comparison of phase-locking value, mean vector length, modulation index, and generalized-linear-modeling-cross-frequency-coupling. *Frontiers in Neuroscience*. 2019; 13:1-15.
- [53] Crandall B, Klein GA, Hoffman RR. Working minds: a practitioner's guide to cognitive task analysis. Mit Press; 2006.
- [54] Salmon P, Stanton NA, Gibbon A, Jenkins D, Walker GH. Human factors methods and sports science: a practical guide. CRC Press; 2009.
- [55] Selim S, Tantawi MM, Shedeed HA, Badr A. A csp\am-ba-svm approach for motor imagery BCI system. *IEEE Access*. 2018; 6:49192-208.
- [56] Sreeja SR, Samanta D. Classification of multiclass motor imagery EEG signal using sparsity approach. *Neurocomputing*. 2019; 368:133-45.
- [57] Sun Y, Xue B, Zhang M, Yen GG. Completely automated CNN architecture design based on blocks. *IEEE transactions on neural networks and learning systems*. 2019; 31(4):1242-54.
- [58] Ma J, Cheng JC, Lin C, Tan Y, Zhang J. Improving air quality prediction accuracy at larger temporal resolutions using deep learning and transfer learning techniques. *Atmospheric Environment*. 2019; 214:1-10.
- [59] Hu L, Zhang Z. EEG signal processing and feature extraction. Singapore: Springer Singapore; 2019.
- [60] Fouladi S, Safaei AA, Mammone N, Ghaderi F, Ebadi MJ. Efficient deep neural networks for classification of Alzheimer's disease and mild cognitive impairment from scalp EEG recordings. *Cognitive Computation*. 2022; 14(4):1247-68.
- [61] Siddiqui F, Mohammad A, Alam MA, Naaz S, Agarwal P, Sohail SS, et al. Deep neural network for EEG signal-based subject-independent imaginary mental task classification. *Diagnostics*. 2023; 13(4):1-23.
- [62] Wen D, Li R, Tang H, Liu Y, Wan X, Dong X, et al. Task-state EEG signal classification for spatial cognitive evaluation based on multiscale high-density convolutional neural network. *IEEE Transactions on Neural Systems and Rehabilitation Engineering*. 2022; 30:1041-51.
- [63] Cui Z, Zheng X, Shao X, Cui L. Automatic sleep stage classification based on convolutional neural network and fine-grained segments. *Complexity*. 2018; 2018:1-14.
- [64] Michielli N, Acharya UR, Molinari F. Cascaded LSTM recurrent neural network for automated sleep stage classification using single-channel EEG signals. *Computers in Biology and Medicine*. 2019; 106:71-81.
- [65] Nagabushanam P, Thomas GS, Radha S. EEG signal classification using LSTM and improved neural network algorithms. *Soft Computing*. 2020; 24:9981-10003.
- [66] Dvorak D, Shang A, Abdel-baki S, Suzuki W, Fenton AA. Cognitive behavior classification from scalp EEG signals. *IEEE Transactions on Neural Systems and Rehabilitation Engineering*. 2018; 26(4):729-39.
- [67] Yıldırım Ö, Baloglu UB, Acharya UR. A deep convolutional neural network model for automated identification of abnormal EEG signals. *Neural Computing and Applications*. 2020; 32:15857-68.
- [68] Ac Çİ, Kaya M, Mishchenko Y. Distinguishing mental attention states of humans via an EEG-based passive BCI using machine learning methods. *Expert Systems with Applications*. 2019; 134:153-66.
- [69] Toa CK, Sim KS, Tan SC. Electroencephalogram-based attention level classification using convolution attention memory neural network. *IEEE Access*. 2021; 9:58870-81.
- [70] Mohanavelu K, Poonguzhali S, Janani A, Vinutha S. Machine learning-based approach for identifying mental workload of pilots. *Biomedical Signal Processing and Control*. 2022.



Hitesh Yadav received his B.Tech degree in Instrumentation Engineering from HNB Garhwal University (A Central University), Srinagar Garhwal, Uttarakhand, India. He received his M.Tech degree in Instrumentation and Control Engineering from Graphic Era University, Dehradun, Uttarakhand. He

has been pursuing his Ph.D. in Electrical and Instrumentation Engineering from Sant Longowal Institute of Engineering and Technology, Longowal, Punjab, India, since 2018. He worked as an Assistant Professor in various Engineering Colleges from 2012 to 2018. His areas of interest are Brain-Computer Interface, EEG, and Biomedical Engineering.

Email: hitesh.yadav125@gmail.com



Surita Maini received her B.Tech degree in Instrumentation Engineering from Dr. B. R. Ambedkar Marathwada University, Maharashtra, India. She received her M. Tech degree in Instrumentation and Control Engineering from Thapar Institute of Engineering and Technology, Patiala, Punjab, India. She received her Ph.D. in Design and Field analysis of EM devices using FEM with application to biomedical problems from Sant Longowal Institute of Engineering and Technology (SLIET), Longowal, Punjab, India. She is currently working as a Professor and Head of the Electrical and Instrumentation Engineering Department of SLIET Longowal. She received the "Shastri Indo Canadian Institute award" for Shastri Mobility Program. She was also visiting faculty at the University of Alberta, Canada. She has several publications in reputed National and International Journals. Her areas of interest are Brain-Computer Interface, Microwave Thermal Ablation, Biomedical Engineering, and Bio-Optics.

Email: suritamaini@gmail.com

Appendix I

S. No.	Abbreviation	Description
1	1D	One Dimensional
2	3D	Three Dimensional
3	AD	Alzheimer Disease
4	BCI	Brain-Computer Interface
5	CAMNN	Convolution Attention Memory Network
6	CFC	Cross-Frequency Coupling
7	CNN	Convolutional Neural Network
8	CSP	Common Spatial Pattern
9	DNN	Deep Neural Network
10	DRNA-Net	Deep Neural Network-Based Dynamic Residual Network
11	ECG	Electrocardiography
12	EEG	Electroencephalogram
13	EMG	Electromyogram
14	ERP	Event-Related Potential
15	fMRI	Functional Magnetic Resonance Imaging
16	FN	False-Negative
17	FP	False-Positive
18	ICA	Independent Component Analysis
19	ISRUC	Institute of System and Robotics, University of Coimbra
20	INN	Improved Neural Network
21	KL	Kullback-Leibler
22	KNN	K-Nearest Neighbour
23	LDA	Linear Discriminant Analysis
24	LS-SVM	Least Square Support Vector Machine
25	LSTM	Long Short-Term Memory Network
26	MAR	Multivariate Autoregressive
27	MBCN	Multi-Branch Convolutional Neural Network
28	MBCN-Bi-LSTM	Multi-Branch Convolutional Neural Network Bi-Directional Long Short-Term Memory Network
29	MCI	Mild Cognitive Impairment
30	MEG	Magnetoencephalography
31	MHCNN	Multiscale High-Density Convolutional Neural Network
32	MI	Modulation Index
33	ML	Machine Learning
34	MLP	Multi-Layer Perceptron
35	PAC	Phase Amplitude Coupling
36	PET	Positron Emission Tomography
37	PSD	Power Spectral Density
38	ReLU	Rectified Linear Unit
39	SAE	Stacked Auto-Encoder
40	SCN	Sequential Convolutional Network
41	STFT	Short-Time Fourier Transform
42	SVM	Support Vector Machine
43	TN	True-Negative
44	TP	True-Positive
45	WT	Wavelet Transform